Vibronic coupling in cyclopentadienyl radical: A method for calculation of vibronic coupling constant and vibronic coupling density analysis

Tohru Sato[a)]
Fukui Institute for Fundamental Chemistry, Kyoto University, Takano-Nishihiraki-cho 34-4, Sakyo-ku, Kyoto 606-8103, Japan and Department of Molecular Engineering, School of Engineering, Kyoto University, Kyoto 615-8510, Japan

Ken Tokunaga
Department of Molecular Engineering, School of Engineering, Kyoto University, Kyoto 615-8510, Japan

Kazuyoshi Tanaka
Department of Molecular Engineering, School of Engineering, Kyoto University, Kyoto 615-8510, Japan and Core Research for Evolutional Science and Technology, Japan Science and Technology Agency (JST-CREST)

A method of calculation of vibronic or electron-phonon coupling constant is presented for a Jahn-Teller molecule, cyclopentadienyl radical. It is pointed out that symmetry breaking at degenerate point and violation of Hellmann-Feynman theorem occur in the calculations based on a single Slater determinant. In order to overcome these difficulties, the electronic wave functions are calculated using generalized restricted Hartree-Fock and complete active space self-consistent-field method and the couplings are computed as matrix elements of the electronic operator of the vibronic coupling. Our result agrees well with the experimental and theoretical values. A concept of vibronic coupling density is proposed in order to explain the order of magnitude of the coupling constant from view of the electronic and vibrational structures. It illustrates the local properties of the coupling and enables us to control the interaction. It could open a way to the engineering of vibronic interactions. © *2006 American Institute of Physics*. [DOI: 10.1063/1.2150816]

I. INTRODUCTION

Vibronic interaction or electron-vibration (phonon) interaction is one of the most investigated problems in molecular physics.[1–4] It plays an important role not only in solid-state physics but also in chemical reaction theory, for instance, Jahn-Teller (JT) effect,[5] superconductivity, electron transfer reaction, and so on. These phenomena are ruled by the magnitude of the vibronic coupling or electron-phonon coupling constant.

Some authors have calculated the vibronic coupling constant from vibronic coupling integrals over hydrogenlike atomic orbitals,[6] and others have evaluated them from the calculation of a conical intersection of Born-Oppenheimer potentials.[7,8] Recently, on the other hand, Kato and Hirao have calculated a vibronic coupling constant of some JT molecules from the gradient of a Born-Oppenheimer potential near the JT crossing point R_0 (see Fig. 1) using density-functional method.[9] However, as we will discuss in this article, their calculations involve some serious problems: (1) symmetry breaking of the wave function and (2) violation of Hellmann-Feynman theorem.[10,11] One of the purposes of this article is to overcome these problems.

Among many JT molecules, cyclopentadienyl radical (C_5H_5, Fig. 2) is one of the most investigated molecule, since it has been not only an important species in organic chemis-

try but also a target of spectroscopy and quantum chemistry. The electronic state of the radical with D_{5h} symmetry is $^2E_1''$, as shown in Fig. 3.

Throughout this article, we consider linear vibronic coupling and neglect higher-order couplings. The JT-active vibrational mode which couples to the electronic E_1'' state can be deduced as

$$[E_1''^2] = a_1' \oplus e_2', \tag{1}$$

where $[\Gamma^2]$ denotes the symmetric product of an irreducible representation Γ. Therefore, the radical should give rise to a JT distortion with e_2' symmetry, and the resulting structure is C_{2v}. The molecule has $3N-6=24$ vibrational modes,

$$\Gamma_{\text{vib}} = 2a_1' \oplus a_2' \oplus 3e_1' \oplus 4e_2' \oplus a_2'' \oplus e_1'' \oplus 2e_2''. \tag{2}$$

Thus the two a_1' modes and four e_2' can couple to the electronic state as long as the linear JT effect is considered.

The JT distortion of the radical has been first observed using electron-spin resonance (ESR) in condensed phase.[12–16] After the ESR observations in condensed phase, the spectroscopy of the isolated radical has been reported.[17–25] After pioneering work by Liehr,[26] theoretical calculations have been piled up.[27–30]

Recently Applegate *et al.* have observed $\tilde{A}\,^2A_2'' \rightarrow \tilde{X}\,^2E_1''$ transition of the radical in detail and calculated observable spectroscopic constants by *ab initio* method.[8] They estimated the vibronic coupling constants for the four e_2' modes from their experiment and calculation. Since their assignment is
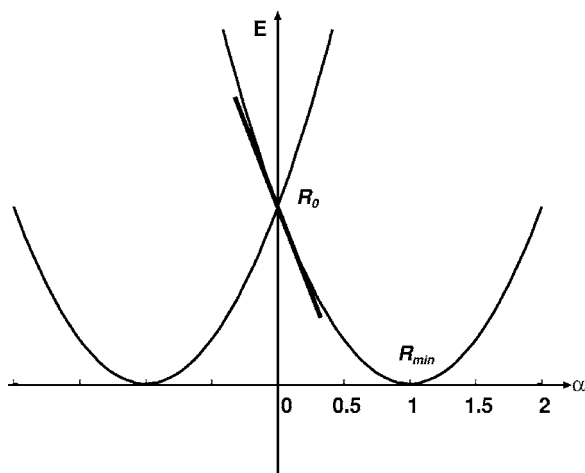

FIG. 1. Cross section of the Jahn-Teller potential. Jahn-Teller crossing $\boldsymbol{R}_0$ is the nuclear configuration of the molecule without Jahn-Teller distortion, and energy minimum $\boldsymbol{R}_{\min}$ is the molecular structure with the lowest energy. The D_{5h} symmetry at $\boldsymbol{R}_0$ is lowered into the C_{2v} at $\boldsymbol{R}_{\min}$ because of the Jahn-Teller effect. For the structure $\boldsymbol{R}_0'$ which is obtained after the optimization for the conical intersection, the energy difference $E_e(\boldsymbol{R}_0') - E_e(\boldsymbol{R}_{\min}) = 1/2D^2$ is called Jahn-Teller stabilization energy ΔE, where D is dimensionless vibronic coupling constant.

quite excellent, cyclopentadienyl radical is a good target for our calculation of the vibronic coupling.

In this paper, we will present a new method of the calculation of the vibronic coupling integrals as matrix elements of an electronic operator of the vibronic couling and compare them with those by Applegate *et al.* Furthermore, we will propose a concept of vibronic coupling density in order to explain the order of magnitude of the coupling constant from view of the electronic and vibrational structures. To find a way to control the coupling is another purpose of this study.

The paper is organized as follows. In Sec. II, the model Hamiltonian of the problem is presented. The method of the calculation is presented in Sec. III. The calculations using the gradient of a Born-Oppenheimer potential at the JT crossing point is not appropriate, since the wave function gives rise to the symmetry breaking at the point. In addition the application of the Hellmann-Feynman theorem that the coupling is equal to the gradient is not valid. We discuss these points in Secs. IV and V, respectively. In Sec. VI, the results of calculations are shown and we discuss the constants in terms of the vibronic coupling density. Finally, we conclude this work in Sec. VII.

II. VIBRONIC HAMILTONIAN
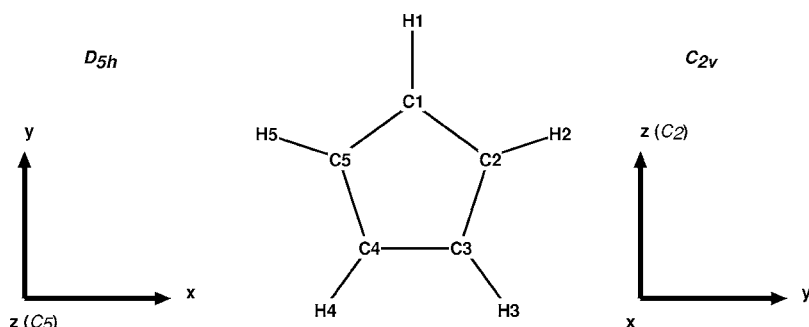
A molecular Hamiltonian is given by

$$\mathcal{H}(r,R) = \mathcal{T}(R) + \mathcal{T}(r) + \mathcal{U}(r,R) = \mathcal{T}(R) + \mathcal{H}_e(r,R), \quad (3)$$

where

$$\mathcal{H}_e(r,R) = \mathcal{T}(r) + \mathcal{U}(r,R), \quad (4)$$

$\boldsymbol{R}$ denotes a set of nuclear coordinates, $\mathbf{r}$ that of electronic coordinates, $\mathcal{T}$ a kinetic-energy operator, and $\mathcal{U}$ a sum of an electron-electron, electronic-nuclear, and nuclear-nuclear potential operator. $\mathcal{H}_e$ is an electronic Hamiltonian which gives a potential surface $E_e(\boldsymbol{R})$ within the Born-Oppenheimer approximation,

$$\mathcal{H}_e(r,R)\phi(r,R) = E_e(\boldsymbol{R})\phi(r,R). \quad (5)$$

Starting from a reference nuclear configuration $\boldsymbol{R}_0$, which is the JT crossing point in the JT problem, the electronic Hamiltonian for a deformed molecule whose nuclear coordinates are expressed by $\boldsymbol{R}$ is written as

$$\mathcal{H}_e(r,R) = \mathcal{H}_e(r,R_0) + \mathcal{U}(r,R) - \mathcal{U}(r,R_0)$$
$$= \mathcal{H}_e(r,R_0) + \Delta\mathcal{U}(r,R). \quad (6)$$

Thus the molecular Hamiltonian is rewritten using the electronic Hamiltonian at $\boldsymbol{R}_0$ as

$$\mathcal{H}(r,R) = \mathcal{T}(R) + \mathcal{H}_e(r,R_0) + \Delta\mathcal{U}(r,R). \quad (7)$$

Since the deformation is expressed in terms of a set of normal coordinates Q_i at $\boldsymbol{R}_0$,

$$\Delta\mathcal{U} = \sum_i \left(\frac{\partial\mathcal{U}}{\partial Q_i}\right)_0 Q_i + \frac{1}{2}\sum_i \left(\frac{\partial^2\mathcal{U}}{\partial Q_i^2}\right)_0 Q_i^2 + \cdots$$
$$(i = 1,2,\ldots,3N-6). \quad (8)$$

Here we ignored intermode couplings so that the vibrations are considered as isolated. This expansion originates from Herzberg-Teller expansion around the JT crossing $\boldsymbol{R}_0$ up to the second order in Q_i. Therefore, the model Hamiltonian describing the coupling between harmonic vibration and electronic motion can be written as

$$\mathcal{H} = \sum_i -\frac{\hbar^2}{2}\left(\frac{\partial^2}{\partial Q_i^2}\right) + \mathcal{H}_e(r,R_0) + \sum_i \left(\frac{\partial\mathcal{U}}{\partial Q_i}\right)_0 Q_i$$
$$+ \sum_i \frac{1}{2}\omega_i^2 Q_i^2, \quad (9)$$

where ω_i is the frequency of the mode. The index i runs over $2a_1' \oplus 4e_2'$ modes. The first term in Eq. (9) corresponds to the nuclear kinetic energy. The operator involved in the third term,
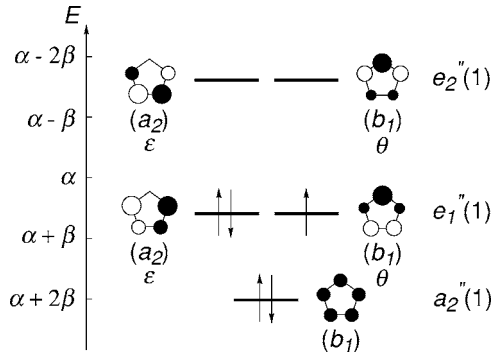

FIG. 2. Structure of cyclopentadienyl radical. Because of the Jahn-Teller effect, symmetry of the structure is lowered from D_{5h} to C_{2v}.

FIG. 3. π orbitals of cyclopentadienyl radical. Because of the fivefold symmetry, the orbital level of HOMO is doubly degenerate e_1'', one of them is denoted as ε, and the other as θ. θ is transformed as yz, and ε is xz. Irreducible representations in the parentheses are those lowered into the subgroup C_{2v}: $E_1'' \downarrow C_{2v} = a_2 \oplus b_1$. ε is a_2 and θ is b_1.

$$V_i = \left(\frac{\partial \mathcal{U}}{\partial Q_i} \right)_0, \tag{10}$$

is called the electronic operator of the mode i, and $V_i Q_i$ describes the vibronic coupling.

The vibronic wave function is expanded in terms of the eigenfunctions of $\mathcal{H}_e(\mathbf{R}_0)$,

$$\Psi(\mathbf{r}, Q) = \sum_n \chi_n(Q) \phi_n(\mathbf{r}, \mathbf{R}_0), \tag{11}$$

where $\phi_n(\mathbf{r}, \mathbf{R}_0)$ is an eigenfunction belonging to the eigenenergy E_0 of $\mathcal{H}_e(\mathbf{R}_0)$ in the electronic eigenequation (5), $\chi_n(Q)$ an expansion coefficient which depends on the normal coordinates, and n runs over the electronic configurations. To obtain a JT Hamiltonian, the domain of n is restricted to the degenerate electronic state $|E_1'' \theta\rangle$, $|E_1'' \varepsilon\rangle$. θ and ε denote one of the irreducible representation of doubly degenerate one that decomposes into b_1 and a_2 when the symmetry is lowered from D_{5h} into C_{2v}, respectively. We treat the model Hamiltonian within the model space spanned by $|E_1'' \theta\rangle$ and $|E_1'' \varepsilon\rangle$. Thus we can write the JT Hamiltonian matrix as follows:

$$\hat{\mathcal{H}}_{JT} = E_0 \hat{\sigma}_0 + \sum_i \left\{ -\frac{\hbar^2}{2} \left(\frac{\partial^2}{\partial Q_i^2} \right) \hat{\sigma}_0 + \frac{1}{2} \omega_i^2 Q_i^2 \hat{\sigma}_0 \right\}$$
$$+ \sum_i \begin{pmatrix} \langle E_1'' \theta | \left(\frac{\partial \mathcal{U}}{\partial Q_i} \right)_0 | E_1'' \theta \rangle & \langle E_1'' \theta | \left(\frac{\partial \mathcal{U}}{\partial Q_i} \right)_0 | E_1'' \varepsilon \rangle \\ \langle E_1'' \varepsilon | \left(\frac{\partial \mathcal{U}}{\partial Q_i} \right)_0 | E_1'' \theta \rangle & \langle E_1'' \varepsilon | \left(\frac{\partial \mathcal{U}}{\partial Q_i} \right)_0 | E_1'' \varepsilon \rangle \end{pmatrix} Q_i \tag{12}$$

$$= \left[E_0 + \sum_i \left\{ -\frac{\hbar^2}{2} \left(\frac{\partial^2}{\partial Q_i^2} \right) + \frac{1}{2} \omega_i^2 Q_i^2 \right\} \right] \hat{\sigma}_0 + \sum_i \hat{V}_i Q_i, \tag{13}$$

where

$$\hat{\sigma}_0 = \begin{pmatrix} 1 & 0 \\ 0 & 1 \end{pmatrix}. \tag{14}$$

The last term in Eq. (13) describes the vibronic coupling. The integrals $\langle E_1'' \theta | (\partial \mathcal{U} / \partial Q_i)_0 | E_1'' \theta \rangle$ and so on are called vi-

bronic coupling integrals (VCIs), which are the matrix elements of the electronic operator V_i.

The coupling matrix between the jth vibrational degenerate e_2' mode and the electronic E_1'' state can be reduced using Wigner-Eckart theorem,

$$\begin{pmatrix} \langle E_1'' \theta | V_{\theta(j)} | E_1'' \theta \rangle & \langle E_1'' \theta | V_{\theta(j)} | E_1'' \varepsilon \rangle \\ \langle E_1'' \varepsilon | V_{\theta(j)} | E_1'' \theta \rangle & \langle E_1'' \varepsilon | V_{\theta(j)} | E_1'' \varepsilon \rangle \end{pmatrix}$$
$$= \frac{1}{\sqrt{2}} \langle E_1'' \| V_{e_2'(j)} \| E_1'' \rangle \begin{pmatrix} \frac{1}{\sqrt{2}} & 0 \\ 0 & -\frac{1}{\sqrt{2}} \end{pmatrix}, \tag{15}$$

and

$$\begin{pmatrix} \langle E_1'' \theta | V_{\varepsilon(j)} | E_1'' \theta \rangle & \langle E_1'' \theta | V_{\varepsilon(j)} | E_1'' \varepsilon \rangle \\ \langle E_1'' \varepsilon | V_{\varepsilon(j)} | E_1'' \theta \rangle & \langle E_1'' \varepsilon | V_{\varepsilon(j)} | E_1'' \varepsilon \rangle \end{pmatrix}$$
$$= \frac{1}{\sqrt{2}} \langle E_1'' \| V_{e_2'(j)} \| E_1'' \rangle \begin{pmatrix} 0 & \frac{1}{\sqrt{2}} \\ \frac{1}{\sqrt{2}} & 0 \end{pmatrix}. \tag{16}$$

Therefore, the reduced matrix element $\langle E_1'' \| V_{e_2'(j)} \| E_1'' \rangle$ can be calculated from the following relations:

$$\langle E_1'' \| V_{e_2'(j)} \| E_1'' \rangle = 2 \langle E_1'' \theta | V_{\theta(j)} | E_1'' \theta \rangle = -2 \langle E_1'' \varepsilon | V_{\theta(j)} | E_1'' \varepsilon \rangle$$
$$= 2 \langle E_1'' \theta | V_{\varepsilon(j)} | E_1'' \varepsilon \rangle = 2 \langle E_1'' \varepsilon | V_{\varepsilon(j)} | E_1'' \theta \rangle. \tag{17}$$

Thus, for a single degenerate vibrational mode, the vibronic coupling matrix is obtained as

$$\hat{V}_{e_2' \theta(j)} = \frac{1}{2} \langle E_1'' \| V_{e_2'(j)} \| E_1'' \rangle \begin{pmatrix} 1 & 0 \\ 0 & -1 \end{pmatrix} = V_{e_2'(j)} \begin{pmatrix} 1 & 0 \\ 0 & -1 \end{pmatrix}, \tag{18}$$

and

$$\hat{V}_{e_2' \varepsilon(j)} = \frac{1}{2} \langle E_1'' \| V_{e_2'(j)} \| E_1'' \rangle \begin{pmatrix} 0 & 1 \\ 1 & 0 \end{pmatrix} = V_{e_2'(j)} \begin{pmatrix} 0 & 1 \\ 1 & 0 \end{pmatrix}, \tag{19}$$

where

$$V_{e_2'(j)} = \frac{1}{2} \langle E_1'' \| V_{e_2'(j)} \| E_1'' \rangle = \langle E_1'' \theta | V_{\theta(j)} | E_1'' \theta \rangle = -\langle E_1'' \varepsilon | V_{\theta(j)}$$
$$\times | E_1'' \varepsilon \rangle = \langle E_1'' \theta | V_{\varepsilon(j)} | E_1'' \varepsilon \rangle = \langle E_1'' \varepsilon | V_{\varepsilon(j)} | E_1'' \theta \rangle \tag{20}$$

is the vibronic coupling constant (VCC), which is the quantity we will calculate in this article.

On the other hand, the interaction matrix between vibrational a_1' mode k is written as

$$\hat{V}_{a_1'(k)} = \begin{pmatrix} \langle E_1'' \theta | V_{a_1'(k)} | E_1'' \theta \rangle & \langle E_1'' \theta | V_{a_1'(k)} | E_1'' \varepsilon \rangle \\ \langle E_1'' \varepsilon | V_{a_1'(k)} | E_1'' \theta \rangle & \langle E_1'' \varepsilon | V_{a_1'(k)} | E_1'' \varepsilon \rangle \end{pmatrix}$$
$$= \frac{1}{\sqrt{2}} \langle E_1'' \| V_{a_1'(k)} \| E_1'' \rangle \begin{pmatrix} 1 & 0 \\ 0 & 1 \end{pmatrix} = V_{a_1'(k)} \begin{pmatrix} 1 & 0 \\ 0 & 1 \end{pmatrix}, \tag{21}$$

where

$$V_{a_1'(k)} = \frac{1}{\sqrt{2}} \langle E_1'' || \mathcal{V}_{a_1'(k)} || E_1'' \rangle = \langle E_1'' \theta | \mathcal{V}_{a_1'(k)} | E_1'' \theta \rangle$$

$$= \langle E_1'' \varepsilon | \mathcal{V}_{a_1'(k)} | E_1'' \varepsilon \rangle \tag{22}$$

is a VCC for a totally symmetric a_1' mode. Therefore, using Eqs. (20) and (22), the VCC can be obtained from a numerical calculation of the VCI. Furthermore Eqs. (20) and (22) involve conditions among the VCI due to the symmetry of the wave function which should be satisfied in the JT system. In Sec. IV, we will discuss the symmetry of wave functions at the degenerate point $\boldsymbol{R}_0$.

We introduce here some dimensionless quantities. For a vibrational mode i, the normal coordinate Q_i is measured by $\sqrt{\hbar/\omega_i}$,

$$Q_i = \sqrt{\frac{\hbar}{\omega_i}} q_i, \tag{23}$$

where q_i is a dimensionless normal coordinate. Dimensionless coupling constant D_i can be defined as

$$D_i = \frac{V_i}{\sqrt{\hbar \omega_i^3}}. \tag{24}$$

Therefore, the JT Hamiltonian is written in terms of these dimensionless quantities:

$$\hat{\mathcal{H}}_{JT} = E_0 \hat{\sigma}_0 + \sum_{k=1}^{2} \left\{ -\frac{\hbar^2}{2} \left(\frac{\partial^2}{\partial Q_{a_1'(k)}^2} \right) \hat{\sigma}_0 + \frac{1}{2} \omega_{a_1'(k)}^2 Q_{a_1'(k)}^2 \hat{\sigma}_0 \right.$$

$$+ Q_{a_1'(k)} V_{a_1'(k)} \hat{\sigma}_0 \Big\} + \sum_{j=1}^{4} \left\{ -\frac{\hbar^2}{2} \left(\frac{\partial^2}{\partial Q_{e_2'(j)\theta}^2} \right) \hat{\sigma}_0 \right.$$

$$- \frac{\hbar^2}{2} \left(\frac{\partial^2}{\partial Q_{e_2'(j)\varepsilon}^2} \right) \hat{\sigma}_0 + \frac{1}{2} \omega_{e_2'(j)}^2 Q_{e_2'(j)\theta}^2 \hat{\sigma}_0$$

$$+ \frac{1}{2} \omega_{e_2'(j)}^2 Q_{e_2'(j)\varepsilon}^2 \hat{\sigma}_0 + V_{e_2'(j)} (Q_{e_2'(j)\theta} \hat{\sigma}_z + Q_{e_2'(j)\varepsilon} \hat{\sigma}_x) \Big\}$$

$$\tag{25}$$

$$= E_0 \hat{\sigma}_0 + \sum_{k=1}^{2} \hbar \omega_{a_1'(k)} \left\{ -\frac{1}{2} \left(\frac{\partial^2}{\partial q_{a_1'(k)}^2} \right) \hat{\sigma}_0 + \frac{1}{2} q_{a_1'(k)}^2 \hat{\sigma}_0 \right.$$

$$+ q_{a_1'(k)} D_{a_1'(k)} \hat{\sigma}_0 \Big\} + \sum_{j=1}^{4} \hbar \omega_{e_2'(j)} \left\{ -\frac{1}{2} \left(\frac{\partial^2}{\partial q_{e_2'(j)\theta}^2} \right) \hat{\sigma}_0 \right.$$

$$- \frac{1}{2} \left(\frac{\partial^2}{\partial q_{e_2'(j)\varepsilon}^2} \right) \hat{\sigma}_0 + \frac{1}{2} q_{e_2'(j)\theta}^2 \hat{\sigma}_0 + \frac{1}{2} q_{e_2'(j)\varepsilon}^2 \hat{\sigma}_0 + D_{e_2'(j)}$$

$$\times (q_{e_2'(j)\theta} \hat{\sigma}_z + q_{e_2'(j)\varepsilon} \hat{\sigma}_x) \Big\}, \tag{26}$$

where

$$\hat{\sigma}_x = \begin{pmatrix} 0 & 1 \\ 1 & 0 \end{pmatrix}, \quad \hat{\sigma}_z = \begin{pmatrix} 1 & 0 \\ 0 & -1 \end{pmatrix}. \tag{27}$$

III. METHOD OF CALCULATION

As the reference structure $\boldsymbol{R}_0$ of the JT system, we take the structure of cyclopentadienyl anion, which is called *parent system* throughout this article. Since the parent system does not give rise to any JT distortion, its geometry has D_{5h} geometry.

The electronic operator $\mathcal{V}_i$ is a sum of one-electron operators $v_i(a)$ and the derivative of the nuclear-nuclear repulsion potential $\mathcal{U}_{nn}$ with respect to Q_i,

$$\mathcal{V}_i = -\sum_a \sum_\alpha \left[\frac{\partial}{\partial Q_i} \left(\frac{Z_\alpha e^2}{|\boldsymbol{r}_a - \boldsymbol{R}_\alpha|} \right) \right]_0 + \frac{\partial \mathcal{U}_{nn}}{\partial Q_i}$$

$$= \sum_a v_i(a) + \frac{\partial \mathcal{U}_{nn}}{\partial Q_i}, \tag{28}$$

where

$$v_i(a) = -\sum_\alpha \left[\frac{\partial}{\partial Q_i} \left(\frac{Z_\alpha e^2}{|\boldsymbol{r}_a - \boldsymbol{R}_\alpha|} \right) \right]_0 = \left(\frac{\partial u(a)}{\partial Q_i} \right)_0, \tag{29}$$

indices α and a denote nucleus and electron, respectively, Z_α charge of the nucleus α, and

$$u(a) = -\sum_\alpha \frac{Z_\alpha e^2}{|\boldsymbol{r}_a - \boldsymbol{R}_\alpha|}. \tag{30}$$

It should be noted that $\partial \mathcal{U}_{nn}/\partial Q_i$ is zero except for the a_1' modes.

The normal coordinate Q_i $(i=1,2,\dots,3N-6)$ is related to $3N$ Cartesian coordinates $\boldsymbol{R}_\alpha = (X_\alpha, Y_\alpha, Z_\alpha) = (R_{3\alpha-2}, R_{3\alpha-1}, R_{3\alpha})$ $(\alpha=1,2,\dots,N)$ by

$$R_\beta = \frac{1}{\sqrt{M_\alpha}} \sum_{i=1}^{3N-6} l_{\beta i} Q_i \quad (\beta=1,2,\dots,3N), \tag{31}$$

where $l_{\beta i}$ can be determined from a vibrational analysis, and M_α denotes the mass of a nucleus α. The one-electron electronic operator $v_i(a)$ is written as

$$v_i(a) = \left(\frac{\partial u(a)}{\partial Q_i} \right)_0 = \sum_{\beta=1}^{3N} \left(\frac{\partial u(a)}{\partial R_\beta} \right)_0 \left(\frac{\partial R_\beta}{\partial Q_i} \right)_0$$

$$= \sum_{\beta=1}^{3N} \left(\frac{\partial u(a)}{\partial R_\beta} \right)_0 \frac{1}{\sqrt{M_\alpha}} l_{\beta i} = \sum_{\beta=1}^{3N} v_\beta(a) l_{\beta i}, \tag{32}$$

where

$$v_\beta(a) = \frac{1}{\sqrt{M_\alpha}} \left(\frac{\partial u(a)}{\partial R_\beta} \right)_0. \tag{33}$$

For the Hartree-Fock (HF) methods, the E_1'' wave functions are written as a single Slater determinant,

$$|E_1''\theta(\text{HF})\rangle = |\cdots \psi_m \alpha \psi_m \beta \cdots \psi_\theta \alpha \psi_\varepsilon \alpha \psi_\varepsilon \beta\rangle =: |\theta\rangle, \tag{34}$$

and

$$|E_1''\varepsilon(\text{HF})\rangle = |\cdots \psi_m \alpha \psi_m \beta \cdots \psi_\theta \alpha \psi_\varepsilon \alpha \psi_\theta \beta\rangle =: |\varepsilon\rangle, \tag{35}$$

where ψ_θ and ψ_ε denote the degenerate highest occupied molecular orbital (HOMO) (see Fig. 3), and α, β are spin functions. The complete active space self-consistent-field (CASSCF) wave functions are written as

$$|E_1'' \theta(\mathrm{CASSCF})\rangle = \sum_I C_{I\theta}|\phi_I\rangle, \tag{36}$$

$$|E_1'' \varepsilon(\mathrm{CASSCF})\rangle = \sum_I C_{I\varepsilon}|\phi_I\rangle, \tag{37}$$

where ϕ_I is a ground or excited electronic configuration within the active space, and C_I is a coefficient.

The vibronic coupling matrices of the HF and CASSCF wave functions are given by

$$\hat{V}_i^{\mathrm{HF}} = \begin{pmatrix} \langle\theta|\mathcal{V}_i|\theta\rangle & \langle\theta|\mathcal{V}_i|\varepsilon\rangle \\ \langle\varepsilon|\mathcal{V}_i|\theta\rangle & \langle\varepsilon|\mathcal{V}_i|\varepsilon\rangle \end{pmatrix}, \tag{38}$$

and

$$\hat{V}_i^{\mathrm{CAS}} = \begin{pmatrix} \displaystyle\sum_{I,I'} C_{I\theta}^* C_{I'\theta}\langle\phi_I|\mathcal{V}_i|\phi_{I'}\rangle & \displaystyle\sum_{I,I'} C_{I\theta}^* C_{I'\varepsilon}\langle\phi_I|\mathcal{V}_i|\phi_{I'}\rangle \\ \displaystyle\sum_{I,I'} C_{I\varepsilon}^* C_{I'\theta}\langle\phi_I|\mathcal{V}_i|\phi_{I'}\rangle & \displaystyle\sum_{I,I'} C_{I\varepsilon}^* C_{I'\varepsilon}\langle\phi_I|\mathcal{V}_i|\phi_{I'}\rangle \end{pmatrix}, \tag{39}$$

respectively. All matrix elements are constructed from the integrals over Slater determinants. In general the integrals of a one-electron operator $\mathcal{O}_1 = \sum_i h(i)$ over Slater determinants are expressed as

$$\langle\cdots mn\cdots|\mathcal{O}_1|\cdots mn\cdots\rangle = \sum_m \langle m|h|m\rangle, \tag{40}$$

$$\langle\cdots mn\cdots|\mathcal{O}_1|\cdots pn\cdots\rangle = \langle m|h|p\rangle, \tag{41}$$

$$\langle\cdots mn\cdots|\mathcal{O}_1|\cdots pq\cdots\rangle = 0, \tag{42}$$

where m, n, p, and q denote spin-orbitals.[31] Since $\mathcal{V}_i$ is a sum of the one-electron operator v_i, the integrals in Eq. (38) can be decomposed as

$$\langle\theta|\mathcal{V}|\theta\rangle = \sum_m n_m\langle\psi_m|v|\psi_m\rangle, \tag{43}$$

$$\langle\theta|\mathcal{V}|\varepsilon\rangle = \langle\psi_\theta|v|\psi_\varepsilon\rangle, \tag{44}$$

$$\langle\varepsilon|\mathcal{V}|\theta\rangle = \langle\psi_\varepsilon|v|\psi_\theta\rangle, \tag{45}$$

$$\langle\varepsilon|\mathcal{V}|\varepsilon\rangle = \sum_m n_m\langle\psi_m|v|\psi_m\rangle, \tag{46}$$

where m runs over the occupied spatial orbitals, and n_m is a occupation number of the orbital m.[31] On the other hand, evaluation of those in Eq. (39) is slightly complicated. The integral $\langle\phi_I|\mathcal{V}|\phi_{I'}\rangle$ is finite if the two configurations differ by less than one spin-orbital, otherwise zero. For instance, for the case that both ϕ_I and $\phi_{I'}$ are single-electron excited configurations, the integral is decomposed as follows:
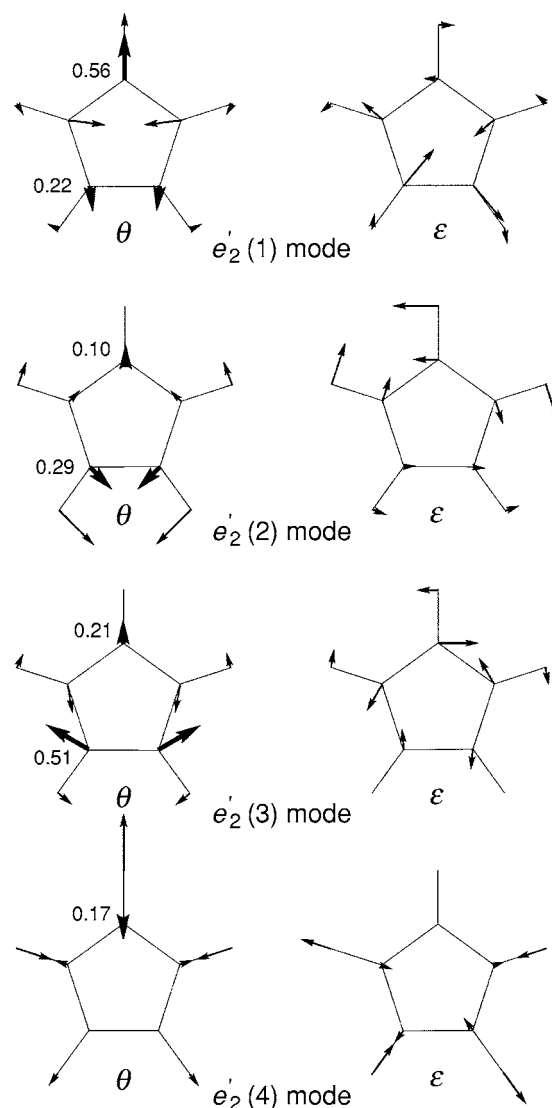

FIG. 4. Jahn-Teller active e_2' vibrational modes. The largest displacement locates on the carbon atoms for $e_2'(1)$ and $e_2'(3)$, and on hydrogen atoms for $e_2'(2)$ and $e_2'(4)$. The displacements of the bold arrows greatly contribute to the VCC. Inserted values are the magnitude of bold arrows. $C_{2v}:E_2'\downarrow C_{2v}$ $=a_1\oplus b_2$. θ is a_1 and ε is b_2.

$$\langle\phi_a^r|\mathcal{V}|\phi_b^s\rangle = \begin{cases} \displaystyle\sum_m \langle\chi_m|v|\chi_m\rangle & \text{if } a=b, \quad r=s \\ \langle\chi_r|v|\chi_s\rangle & \text{if } a=b, \quad r\neq s \\ -\langle\chi_a|v|\chi_b\rangle & \text{if } a\neq b, \quad r=s \\ 0 & \text{if } a\neq b, \quad r\neq s, \end{cases} \tag{47}$$

where χ_a and χ_b denote occupied spin-orbitals, and χ_r and χ_s unoccupied spin-orbitals. m runs over the occupied spin-orbitals.

The VCI over Slater determinants $|\theta\rangle$ and $|\varepsilon\rangle$ can be decomposed into orbital vibronic integrals (OVCIs) for the θ mode over molecular orbitals,

$$\langle\theta|\mathcal{V}_\theta|\theta\rangle = -\langle\varepsilon|\mathcal{V}_\theta|\varepsilon\rangle = \sum_{m\in E_1'\oplus E_1''} \{n_{\theta(m)}\langle\psi_{\theta(m)}|v_\theta|\psi_{\theta(m)}\rangle + n_{\varepsilon(m)}\langle\psi_{\varepsilon(m)}|v_\theta|\psi_{\varepsilon(m)}\rangle\}, \tag{48}$$

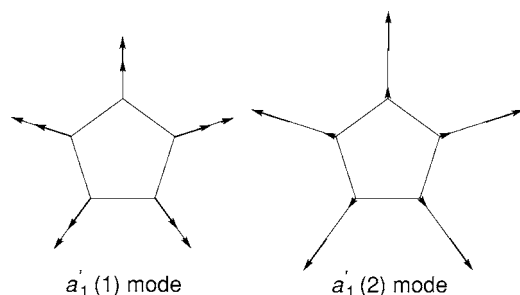where m runs over the occupied molecular orbitals with or-

FIG. 5. Totally symmetric a_1' vibrational modes. The largest displacement locates on the carbon atoms for $a_1'(1)$, and on hydrogen atoms for $a_1'(2)$.

bital E_1' and E_1'' symmetry, and $\psi_{\theta(m)}$ and $\psi_{\varepsilon(m)}$ denote the degenerate pair of the E_1' or E_1' spatial orbitals. $n_{\theta(m)}$ and $n_{\theta(m)}$ are occupation numbers of $\psi_{\theta(m)}$ and $\psi_{\varepsilon(m)}$. Note that all the orbitals with the E_1' symmetry can also couple to the E_2' mode since $[E_1'^2]=A_1'\oplus E_2'$. Furthermore it should be noted here that

$$\langle\psi_{\theta(m)}|v_\theta|\psi_{\theta(m)}\rangle+\langle\psi_{\varepsilon(m)}|v_\theta|\psi_{\varepsilon(m)}\rangle=0, \quad (49)$$

because of the symmetry of the matrix elements as appeared in Eq. (17). Therefore, contributions from a pair of $\psi_{\theta(m)}$ and $\psi_{\varepsilon(m)}$ are canceled and the vibronic coupling integrals can be reduced into OVCI over the doubly occupied frontier orbitals ψ_θ or ψ_ε,

$$\langle\theta|\mathcal{V}_{\theta(j)}|\theta\rangle=\langle\psi_\varepsilon|v_{\theta(j)}|\psi_\varepsilon\rangle,$$
$$\langle\varepsilon|\mathcal{V}_{\theta(j)}|\varepsilon\rangle=\langle\psi_\theta|v_{\theta(j)}|\psi_\theta\rangle. \quad (50)$$

On the other hand, the VCI for the ε mode is written as

$$\langle\theta|\mathcal{V}_{\varepsilon(j)}|\varepsilon\rangle=\langle\psi_\varepsilon|v_{\varepsilon(j)}|\psi_\theta\rangle,$$
$$\langle\varepsilon|\mathcal{V}_{\varepsilon(j)}|\theta\rangle=\langle\psi_\theta|v_{\varepsilon(j)}|\psi_\varepsilon\rangle. \quad (51)$$

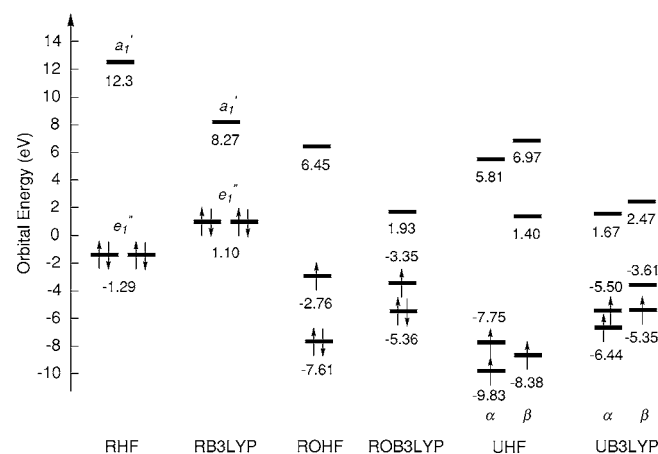Therefore, the vibronic coupling matrix in the HF methods is equal to the OVCI matrix,

FIG. 6. Incorrect symmetry breaking of the frontier orbitals in cyclopentadienyl radical with D_{5h} symmetry. The left two diagrams are those of cyclopentadienyl anion, and the remaining ones are those of cyclopentadienyl radical. The HOMO should be degenerate because of the high symmetry. However, the HOMO calculated by the methods based on a single determinant, ROHF, ROB3LYP, UHF, and UB3LYP exhibit symmetry breaking.
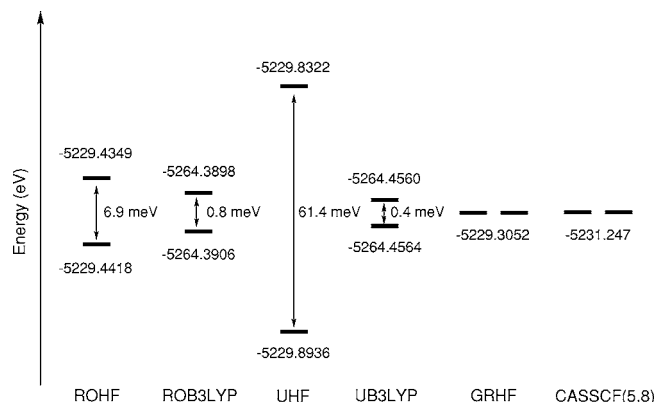

FIG. 7. Calculated electronic state of cyclopentadienyl radical $^2E_1''$ state. Though the results using GRHF and state-averaged CASSCF give correct degeneracy, the calculations using ROHF, ROB3LYP, UHF, and UB3LYP exhibit an incorrect energy splitting.

$$\hat{V}_\theta^{HF}=\begin{pmatrix}\langle\psi_\varepsilon|v_\theta|\psi_\varepsilon\rangle & 0\\ 0 & \langle\psi_\theta|v_\theta|\psi_\theta\rangle\end{pmatrix}, \quad (52)$$

and

$$\hat{V}_\varepsilon^{HF}=\begin{pmatrix}0 & \langle\psi_\theta|v_\varepsilon|\psi_\varepsilon\rangle\\ \langle\psi_\varepsilon|v_\varepsilon|\psi_\theta\rangle & 0\end{pmatrix}. \quad (53)$$

As for the a_1' modes, there is no such cancellation;

$$V_{a_1'(k)}=\langle\theta|\mathcal{V}_{a_1'(k)}|\theta\rangle=\langle\varepsilon|\mathcal{V}_{a_1'(k)}|\varepsilon\rangle=\sum_m\langle\chi_m|v_{a_1'(k)}|\chi_m\rangle$$
$$+\frac{\partial\mathcal{U}_{nn}}{\partial Q_{a_1'(k)}}=\sum_{m'}\langle\chi_{m'}|v_{a_1'(k)}|\chi_{m'}\rangle+\frac{\partial\mathcal{U}_{nn}}{\partial Q_{a_1'(k)}}, \quad (54)$$

where m and m' run over the occupied spin-orbitals of $|\theta\rangle$ and $|\varepsilon\rangle$, respectively.

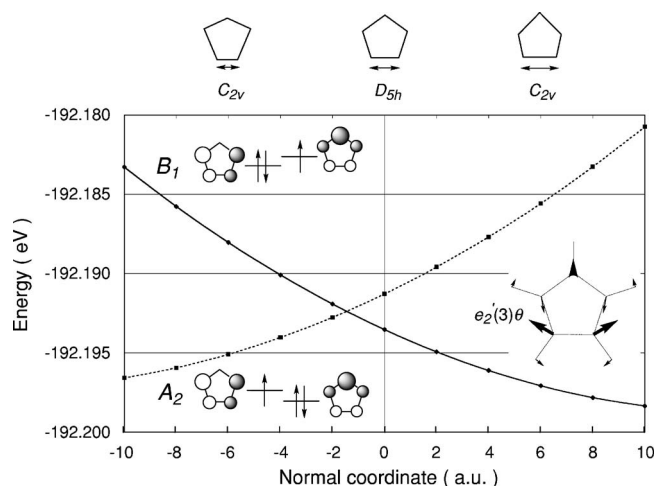Using $l_{\beta i}$ in Eq. (31), the VCC for the e_2' mode can be written as

FIG. 8. Energy curves of the A_2 and B_1 states along the $e_2'(3)$ mode [UHF/6−31G(d,p)]. The Jahn-Teller crossing is disappeared at $Q=0$ where the two energy curves should cross.
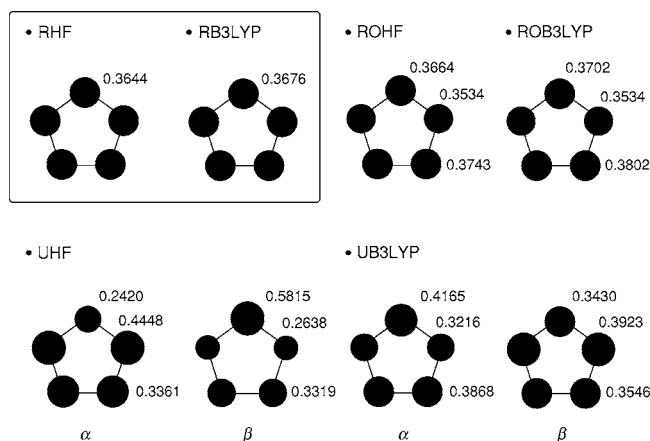
FIG. 9. Symmetry breaking in the lowest π orbital of cyclopentadienyl radical and the anion (framed). The calculations were performed for the D_{5h} structure. The symmetric π orbital $a_2''(1)$ becomes asymmetric when a single-determinant-based calculation is applied. This gives rise to the vibronic coupling matrix with a wrong symmetry (see text). The calculations were performed using STO-3G basis set.

$$V_j = \langle E_1'' \theta | v_{\theta(j)} | E_1'' \theta \rangle \qquad (55)$$

$$= \sum_{\beta=1}^{3N} l_{\beta\theta(j)} \langle E_1'' \theta | v_\beta | E_1'' \theta \rangle \qquad (56)$$

$$= \sum_{\beta=1}^{3N} u_\beta l_{\beta\theta(j)} \qquad (57)$$

$$= K \sum_{\beta=1}^{3N} x_{d\beta} l_{\beta\theta(j)} \qquad (58)$$

$$= K k_j, \qquad (59)$$

where

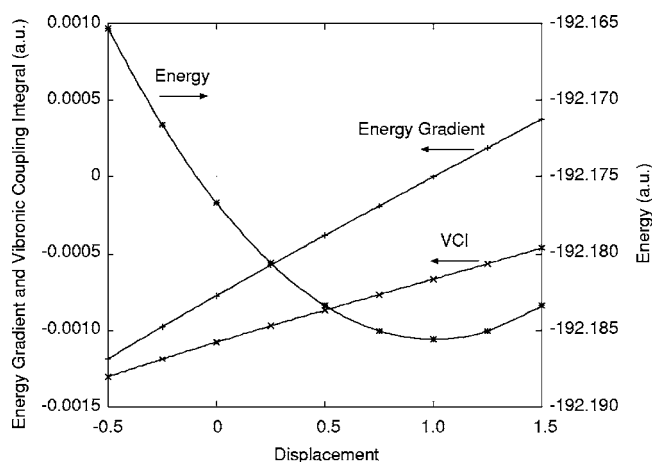$$u_\beta = \langle E_1'' \theta | v_\beta | E_1'' \theta \rangle, \qquad (60)$$

FIG. 10. Energy gradient $\partial E/\partial R$ and $\langle \partial \mathcal{H}/\partial R \rangle$ (VCI in the figure) using ROHF towards the minimum of the potential on the $^2A_2$ manifold. The unity of the displacement corresponds to that between the minimum of the potential and the origin, the Jahn-Teller crossing. The absolute value of $\langle \partial \mathcal{H}/\partial R \rangle$ at the Jahn-Teller crossing is larger than that of the energy gradient.

FIG. 11. Energy gradient $\partial E/\partial R$ and $\langle \partial \mathcal{H}/\partial R \rangle$ (VCI in the figure) using ROB3LYP towards the minimum of the potential on the $^2A_2$ manifold. The unity of the displacement corresponds to that between the minimum of the potential and the origin, the Jahn-Teller crossing. The absolute value of $\langle \partial \mathcal{H}/\partial R \rangle$ at the Jahn-Teller crossing is larger than that of the energy gradient.
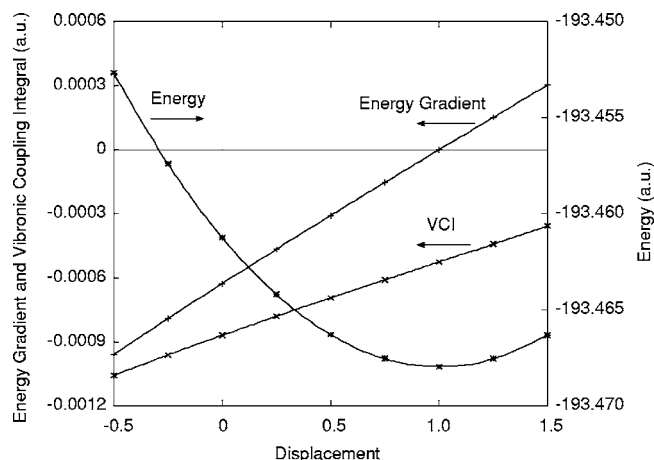
distortion vector x_d is the unit vector in the direction of $u = (u_\beta)$;

$$k_j = \sum_{\beta=1}^{3N} x_{d\beta} l_{\beta\theta(j)}, \qquad (61)$$

and K is a constant. The value of x_d is obtainable from the OVCI. Vibrational analysis yields the value of $l_{\beta\theta(j)}$, and k_j can be calculated from these quantities. The value of K is calculated from a JT stabilization energy, i.e., reorganization energy ΔE,

$$\Delta E \approx \sum_{j=1}^{4} \frac{V_j^2}{2\omega_j^2} = K^2 \sum_{j=1}^{4} \frac{k_j^2}{2\omega_j^2}. \qquad (62)$$

Therefore,

$$K^2 = \Delta E \left(\sum_{j=1}^{4} \frac{k_j^2}{2\omega_j^2} \right)^{-1}, \qquad (63)$$

where ΔE is the difference between the minimum energy of the radical optimized within C_{2v} symmetry and that of conical intersection optimized within D_{5h} symmetry.[7]

In order to obtain the optimized geometry R_0 and vibrational structure of the parent system, restricted Hartree-Fock (RHF) method is employed for cyclopentadienyl anion. At the geometry R_0, we employed state-averaged CASSCF method using GAUSSIAN 98 (Ref. 32) and generalized restricted Hartree-Fock (GRHF) method using CADPAC (Ref. 33) to determine the wave function of cyclopentadienyl radical. All calculations were performed using the 6-31G(d,p) basis set. The VCI was evaluated using these wave functions.

From the results of the electronic structure calculation for the radical at R_0 and the vibrational analysis for the anion, we calculated u and x_d, using Eq. (60). $l_{\beta i}$ is obtained from the vibrational analysis, and k_i was calculated from Eq. (61). K was obtained using Eq. (63) from the results of the

TABLE I. Bond length (Å) of cyclopentadienyl anion $C_5H_5^-$ calculated using RHF/6-31G(d,p) and the neutral radical using GRHF/6-31G(d,p). Note that the geometrical structure employed throughout this work is that of the anion.

Species	Method	C–C	C–H
Anion	RHF/6-31G(d,p)	1.4021	1.0800
Neutral	GRHF/6-31G(d,p)	1.4037	1.0725

calculation of the JT stabilization energy. Scaled V_i was calculated from Eq. (59) using K, and unscaled V_i from Eq. (56).

In the vibrational analysis, positive directions of the normal coordinates are defined in Figs. 4 and 5. All quantities are given in a.u. except for bond lengths and wave numbers throughout this article. The a.u. of the VCC is $m_e^{3/2}e^6/(4\pi\varepsilon_0)^3\hbar^4 = 8.632\ 09 \times 10^7$ J/kg$^{1/2}$ m in the Systéme International (SI) unit.

IV. SYMMETRY BREAKING AND WIGNER-ECKART THEOREM

Figure 6 shows the energy levels of the frontier orbitals calculated using RHF and RB3LYP for the anion and ROHF, ROB3LYP, UHF, and UB3LYP for the neutral radical. As for the anion which has a closed shell, the calculations give a degenerate e_1'' HOMO with the correct degeneracy. However, either in HF or in density-functional theory (DFT) calculations, the restricted open-shell and unrestricted calculations exhibit symmetry broken orbitals for the radical which should have the degenerate e_1'' orbitals. The orbital symmetry cannot be assigned within the D_{5h} point group. It is known that such an incorrect symmetry breaking of the orbitals sometimes occurs in the system involving a degenerate electronic state when a calculation is based on a single determinant.[34] We confirmed the same situation in the present calculation.

Figure 7 shows the calculated total energy of the electronic $^2E_1''$ state for the radical. Since the electronic $^2E_1''$ is degenerate, the total energy of two electronic configurations, $(\psi_\theta)^2(\psi_\varepsilon)^1$ and $(\psi_\theta)^1(\psi_\varepsilon)^2$, should be equal. However, the calculations using ROHF, ROB3LYP, UHF, and UB3LYP exhibit incorrect energy splittings, while the results using GRHF and state-averaged CASSCF give correct degeneracy. Moreover, as shown in Fig. 8, the JT crossing point is disappeared at the point $Q=0$ where the two energy curves should cross.

Symmetry breaking is observed not only in the energy but also in the wave function. Figure 9 illustrates the examples of the symmetry broken orbital of cyclopentadienyl

radical with the D_{5h} symmetry. The lowest π orbital, which should be a_2'' symmetry within the D_{5h} geometry, becomes asymmetric when a single-determinant-based calculation, such as ROHF, ROB3LYP, UHF, and UB3LYP, is applied for the radical.

This gives rise to the vibronic coupling matrix with a wrong symmetry. From Eq. (17), $\langle E_\varepsilon|V_{e_\theta}|E_\varepsilon\rangle$ has the same absolute value as $\langle E_\theta|V_{e_\theta}|E_\theta\rangle$. However, the calculation of the coupling for the $e_2'(3)$ mode using the ROHF wave function yields $\langle E_\theta|V_{e_\theta}|E_\theta\rangle = 0.000\ 941\ 324\ 7$ and $\langle E_\varepsilon|V_{e_\theta}|E_\varepsilon\rangle = -0.000\ 976\ 415\ 9$, and the ROB3LYP calculation gives $\langle E_\theta|V_{e_\theta}|E_\theta\rangle = 0.000\ 801\ 507\ 4$ and $\langle E_\varepsilon|V_{e_\theta}|E_\varepsilon\rangle = -0.000\ 803\ 151\ 2$. Therefore, the symmetry broken orbitals give rise to a symmetry broken interaction matrix. In other words, as for the wave function obtained by ROHF and ROB3LYP, the Wigner-Eckart theorem is not satisfied.

V. HELLMANN-FEYNMAN THEOREM AND ENERGY GRADIENT

The Hellmann-Feynman theorem[10,11] states that, when a Hamiltonian depend on a parameter λ, the derivative of the energy with respect to the parameter is equal to the expectation value of the derivative of the Hamiltonian with respect to λ,

$$\frac{\partial E(\lambda)}{\partial \lambda} = \left\langle \frac{\partial \mathcal{H}(\lambda)}{\partial \lambda} \right\rangle. \qquad (64)$$

If the normal coordinate Q is taken for the parameter λ,

$$\frac{\partial E(Q)}{\partial Q} = \left\langle \frac{\partial \mathcal{H}(Q)}{\partial Q} \right\rangle = \left\langle \frac{\partial \mathcal{U}(Q)}{\partial Q} \right\rangle. \qquad (65)$$

Therefore, if we had applied the theorem for the problem, the VCC could be calculated as the derivative of energy with respect to Q. However, we cannot resort to the Hellmann-Feynman theorem for the calculation of the VCC, because the Hellmann-Feynman theorem is not valid in the present calculations.

Figures 10 and 11 demonstrate that the energy gradient $\partial E/\partial R$ is not equal to the Hellmann-Feynman force $\langle \partial H/\partial R\rangle$ along the path towards the minimum of the potential on the $^2A_2$ manifold in C_{2v} $(^2E_1'' \downarrow C_{2v} = {}^2A_2 \oplus {}^2B_1, C_{2v} \subset D_{5h})$, where the calculations were performed using ROHF and ROB3LYP, respectively. The unity of the displacement corresponds to that between the minimum of the potential and the origin, the JT crossing. In both calculations, the absolute value of the Hellmann-Feynman force at the JT crossing is larger than that of the energy gradient. Therefore, we cannot calculate the vibronic coupling from the energy gradient.

TABLE II. Wave number (cm^{-1}) of cyclopentadienyl anion calculated using RHF/6-31G(d,p) and the neutral radical calculated using GRHF/6-31G(d,p). Experimental values are taken from Ref. 8.

Species	Method	$a_1'(1)$	$a_1'(2)$	$e_2'(1)$	$e_2'(2)$	$e_2'(3)$	$e_2'(4)$
Anion	RHF	1233	3321	914	1144	1497	3263
Neutral	GRHF	1236	3349	918	1198	1596	3313
	Expt.	1071		872	1041	1320	

TABLE III. Total energy and unscaled vibronic coupling constant V (10^{-4} a.u.) of C_5H_5. Basis set employed is 6-31G(d,p). The vibrational vectors are obtained by RHF/6-G(d,p) for the anion.

C_5H_5	RHF	GRHF	CAS(3,4)	CAS(5,5)	CAS(5,6)	CAS(5,8)
Energy	-192.1430[a]	-192.1719	-192.1952	-192.2357	-192.2379	-192.2433
$a_1'(1)$	-31.26	3.49	2.82	1.13	1.17	1.39
$a_1'(2)$	22.63	2.67	2.45	1.87	1.89	1.99
$e_2'(1)$	9.00	8.76	6.50	4.78	4.83	5.09
$e_2'(2)$	13.53	13.60	13.27	11.63	11.58	11.62
$e_2'(3)$	-14.16	-14.61	-15.38	-14.58	-14.50	-14.18
$e_2'(4)$	-7.85	-7.83	-4.95	-3.20	-3.34	-3.34

[a]The energy is estimated using Koopmans' theorem. The energy of the anion is -192.1903 a.u., and HOMO energy is -0.0473.

We confirmed that the Hellmann-Feynman theorem is also violated as well as the Wigner-Eckart theorem. This is the reason why we compute the VCC from the VCI employing the wave function based on the GRHF and state-averaged CASSCF calculation.

VI. RESULTS AND DISCUSSION

A. Geometrical and vibrational structures

The optimized symmetry of the parent system $C_5H_5^-$ and that of the conical intersection for the neutral radical C_5H_5 are D_{5h}. In Table I, the bond lengths of the anion and the neutral radical are tabulated. It is found that the optimized geometries of the energy minimum for the anion and the conical intersection for the radical are almost the same. The bond lengths differ within 0.002 Å for C–C and 0.01 Å for the C–H bond. Thus we take the geometry of the anion as that of the JT crossing point in order to reduce computational resources.

The calculated and experimental[8] vibrational frequencies are summarized in Table II. The calculated vibrational structures are also the same. Therefore, we took the geometrical and vibrational structures of the anion as those of the JT crossing of the radical throughout this study.

B. Vibronic interaction matrix and Wigner-Eckart theorem

The vibronic coupling matrix for the $e_2'(3)$ vibrational mode calculated by RHF is obtained as

$$\begin{pmatrix} \langle E_\theta|V_{e_\theta}|E_\theta\rangle & \langle E_\theta|V_{e_\theta}|E_\varepsilon\rangle \\ \langle E_\varepsilon|V_{e_\theta}|E_\theta\rangle & \langle E_\varepsilon|V_{e_\theta}|E_\varepsilon\rangle \end{pmatrix} = \begin{pmatrix} 0.001\,416\,302\,4 & 0.000\,000\,000\,0 \\ 0.000\,000\,000\,0 & -0.001\,416\,302\,4 \end{pmatrix},$$

and

$$\begin{pmatrix} \langle E_\theta|V_{e_\varepsilon}|E_\theta\rangle & \langle E_\theta|V_{e_\varepsilon}|E_\varepsilon\rangle \\ \langle E_\varepsilon|V_{e_\varepsilon}|E_\theta\rangle & \langle E_\varepsilon|V_{e_\varepsilon}|E_\varepsilon\rangle \end{pmatrix} = \begin{pmatrix} 0.000\,000\,000\,0 & 0.001\,416\,302\,4 \\ 0.001\,416\,302\,4 & 0.000\,000\,000\,0 \end{pmatrix}.$$

TABLE IV. Unscaled dimensionless vibronic coupling constant D of C_5H_5 calculated using 6-31G(d,p) basis set. The vibrational vectors employed in these calculations were obtained with RHF/6-31G(d,p) for the anion. The values outside the parentheses were calculated using the vibrational frequencies of the anion obtained by RHF/6-31G(d,p), and the values in the parentheses using the vibrational frequencies of the radical evaluated by GRHF/6-31G(d,p). Negative signs are neglected.

C_5H_5	RHF	GRHF	CAS(3,4)	CAS(5,5)	CAS(5,6)	CAS(5,8)
$a_1'(1)$	7.42(7.40)	0.83(0.83)	0.67(0.67)	0.27(0.27)	0.28(0.28)	0.33(0.33)
$a_1'(2)$	1.22(1.20)	0.14(0.14)	0.13(0.13)	0.10(0.10)	0.10(0.10)	0.11(0.11)
$e_2'(1)$	3.35(3.33)	3.26(3.24)	2.42(2.40)	1.78(1.77)	1.80(1.79)	1.89(1.88)
$e_2'(2)$	3.59(3.35)	3.61(3.37)	3.53(3.29)	3.09(2.88)	3.08(2.87)	3.09(2.88)
$e_2'(3)$	2.51(2.28)	2.59(2.36)	2.73(2.48)	2.59(2.35)	2.57(2.34)	2.52(2.29)
$e_2'(4)$	0.43(0.42)	0.43(0.42)	0.27(0.27)	0.18(0.17)	0.18(0.18)	0.18(0.18)

TABLE V. Dimensionless scaled vibronic coupling constants for the degenerate e'_2 modes calculated by CASSCF(5,8)/6-31G(d,p). Negative signs are neglected. The calculations 1–3 and experimental values are taken from Ref. 8.

	$D_{e'_2(1)}$	$D_{e'_2(2)}$	$D_{e'_2(3)}$	$D_{e'_2(4)}$
This work	0.79	1.30	1.06	0.08
Calculation 1	0.77	0.98	1.40	<0.14
Calculation 2	0.66	0.82	1.17	<0.14
Calculation 3	0.85	0.82	1.14	<0.14
Experimental	0.62	1.07	0.85	0

Since it has the correct symmetry which is expected from the Wigner-Eckart theorem, we can obtain the vibronic coupling constant $1/2\langle E\|V\|E\rangle = 0.001\,416$. Furthermore we confirmed that the GRHF and CASSCF wave functions satisfy the Wigner-Eckart theorem as well as the RHF wave function.

C. Vibronic coupling constant

The calculated VCCs by RHF, GRHF, and CASSCF methods are tabulated in Table III. These methods yield the appropriate wave function with the correct symmetry. Note that the RHF wave function is not variationally optimized for the radical since the RHF calculation was performed for the parent system, cyclopentadienyl anion. For the a'_1 modes, the RHF wave function yields quite large value, comparing with the variationally optimized wave function. This is because all the occupied orbitals contribute to the VCC of the a'_1 modes, and the errors are accumulated, while only frontier e''_1 orbitals contribute to that of e'_2 modes.

In each calculation, the VCC of the $e'_2(3)$ mode has the largest value of all the e'_2 modes. All calculations show the tendency, $e'_2(3) > e'_2(2) > e'_2(1) > e'_2(4)$, and this agrees with the experimental result. In other words, as long as we are interested in a qualitative aspect of the e'_2 modes, we can employ the RHF wave function for the VCC calculation.

Table IV shows the dimensionless vibronic coupling constant D, which is calculated using the frequency. Though
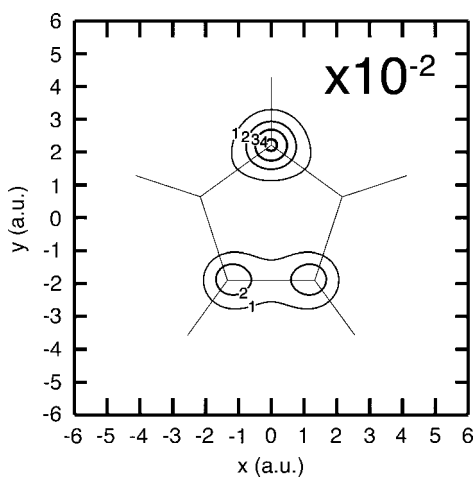

FIG. 12. Contour plot on the plane $z=1.0$ of the electron density $\rho_\theta(\mathbf{r})$ of the frontier $e''_1 \theta$ orbital calculated by the GRHF/6−31G(d,p) method.
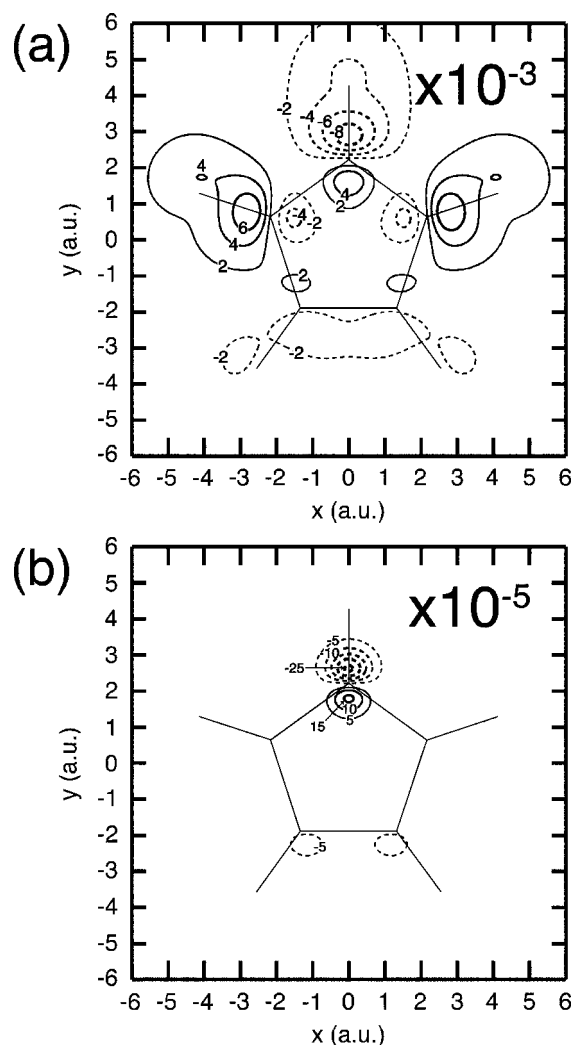

FIG. 13. (a) Contour map on the plane $z=1.0$ of the one-electron vibronic coupling operator $v_\theta(\mathbf{r})$ with respect to the $e'_2(1)\theta$ mode (a.u.). (b) Contour map on the plane $z=1.0$ of the vibronic coupling density $\eta_{e'_2(1)\theta}(\mathbf{r})$ (a.u.).

D calculated by the GRHF frequency is smaller than that calculated by the RHF frequency, the difference is rather small.

The calculated D after the scaling using the constant K is tabulated in Table V. Table V demonstrates good agreement of the present results with the calculation and experiment reported by Applegate *et al.*[8]

D. Vibronic coupling density analysis

Since we have the explicit expressions for the coupling integral, Eq. (52), as discussed in Sec. III, we can discuss VCC in terms of the electronic and vibrational structures. In particular, for the HF wave functions, we can define vibronic coupling density $\eta_j(\mathbf{r})$ in a simple form to analyze the VCC.

Vibronic coupling density $\eta_j(\mathbf{r})$ for the $e'_2(j)$ mode is defined by

$$\eta_j(\mathbf{r}) = \psi_\theta^*(\mathbf{r})\psi_\theta(\mathbf{r})v_{\theta(j)}(\mathbf{r}) = \rho_\theta(\mathbf{r})v_{\theta(j)}(\mathbf{r}), \qquad (66)$$

where $\rho_\theta(\mathbf{r})$ is the frontier electron density of the molecular orbital ψ_θ, and $v_{\theta(j)}(\mathbf{r})$ the one-electron electronic operator defined in Eq. (32). The VCC is written as
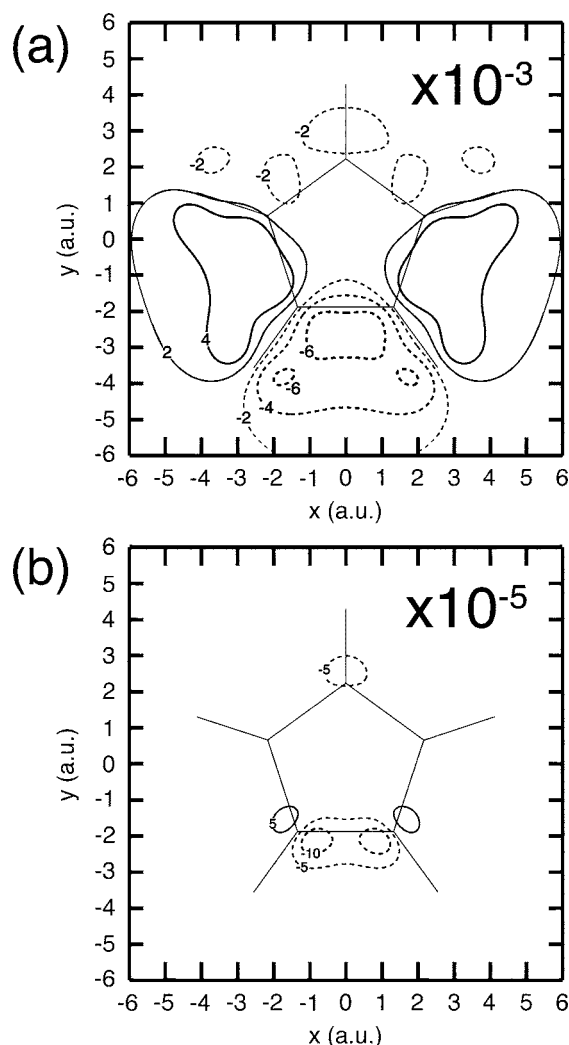
FIG. 14. (a) Contour map on the plane $z=1.0$ of the one-electron vibronic coupling operator $v_\theta(\mathbf{r})$ with respect to the $e_2'(2)\theta$ mode (a.u.). (b) Contour map on the plane $z=1.0$ of the vibronic coupling density $\eta_{e_2'(2)\theta}(\mathbf{r})$ (a.u.).
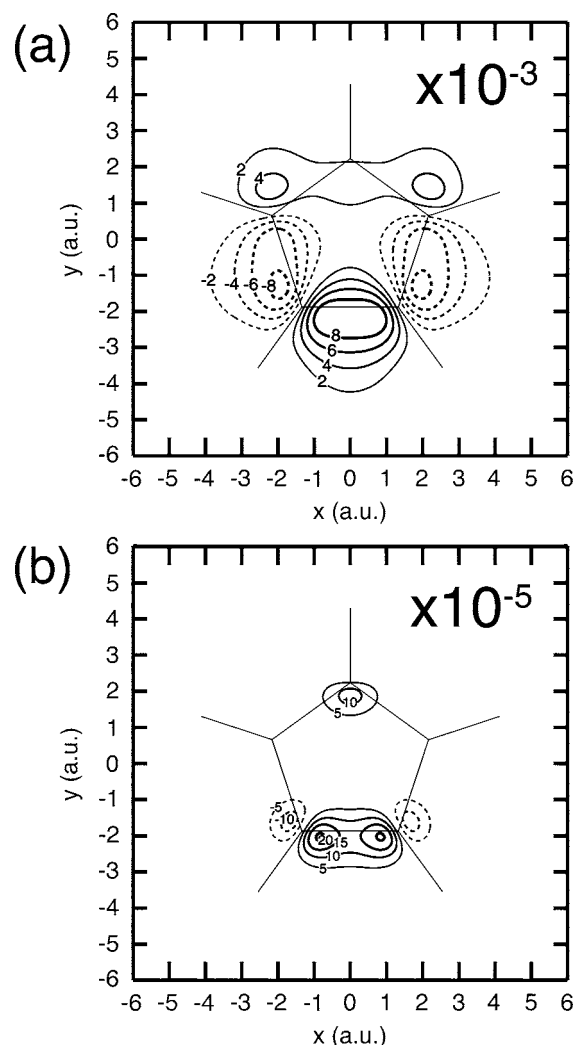
FIG. 15. (a) Contour map on the plane $z=1.0$ of the one-electron vibronic coupling operator $v_\theta(\mathbf{r})$ with respect to the $e_2'(3)\theta$ mode (a.u.). (b) Contour map on the plane $z=1.0$ of the vibronic coupling density $\eta_{e_2'(3)\theta}(\mathbf{r})$ (a.u.).

$$V_j = \int d\mathbf{r}\, \eta_j(\mathbf{r}). \tag{67}$$

The vibronic coupling density enables us to analyze the calculated VCC in terms of the electronic structure $\rho_\theta(\mathbf{r})$ and the derivative of the potential with respect to the normal coordinate $v_{\theta(j)}(\mathbf{r})$.

In Fig. 4, the JT-active e_2' modes are shown. It should be noted that the larger components of the vibrational modes lie on the carbon atoms for $e_2'(1)$ and $e_2'(3)$, while the hydrogens in $e_2'(2)$ or $e_2'(4)$ have large contribution.

Figure 12 shows the contour plot of the frontier electron density $\rho_\theta(\mathbf{r})$ of $e_1''\theta$ orbital calculated from the GRHF wave function (see Fig. 3).

In Fig. 13(a), the derivative of the potential with respect to the $e_2'(1)\theta$ mode is shown. It is found that the large values are distributed on the C1–H1, C2–H2, and C5–H5 bonds. However, there is little electron density on the C2–H2 and C5–H5 bonds. Consequently, the vibronic coupling density of this mode η_1 is small and negative, and localized on the C1–H1 bond, as shown in Fig. 13(b).

Figure 14(a) shows the derivative of the potential with

respect to the $e_2'(2)\theta$ mode. The derivative of the potential has a large value not just on the C–C bonds but near the C3–C4, C2–C3, and C4–C5 bonds. This is because the large displacement of this mode lies on the hydrogen atoms. Since the electron density is localized on the C3–C4 bond, the vibronic coupling density for this mode η_2 gives rather large near the C3–C4 bond as shown in Fig. 14(b).

The derivative of the potential with respect to the $e_2'(3)\theta$ mode is shown in Fig. 15(a). This mode yields the largest VCC among the four. The derivative plot shows a distribution on the C3–C4, C2–C3, and C4–C5 bonds. Figure 14(b) shows the vibronic coupling density η_3. As the result of the electron and derivative potential distributions, η_3 is distributed in the region near the C3–C4 bond. The broad distribution makes the VCC of this mode large. The coincidence between the electron density distribution ρ_θ and the distribution of the derivative potential is the reason why the VCC of the $e_2'(3)\theta$ mode is the largest of the four.

In Fig. 16(a), the derivative potential with respect to the $e_2'(4)\theta$ mode is shown. It is distributed on the C1–H1, C2–H2, and C5–H5 bonds where ρ_θ gives small value. The vibronic coupling density of this mode [Fig. 16(b)] illustrates
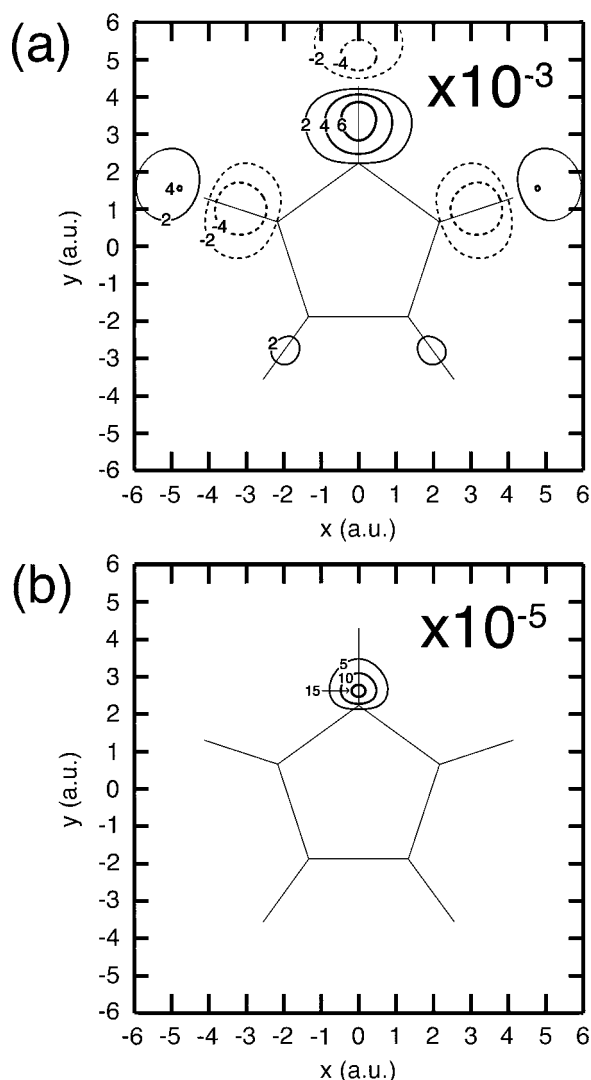
FIG. 16. (a) Contour map on the plane $z=1.0$ of the one-electron vibronic coupling operator $v_\theta(\mathbf{r})$ with respect to the $e_2'(4)\theta$ mode (a.u.). (b) Contour map on the plane $z=1.0$ of the vibronic coupling density $\eta_{e_2'(4)\theta}(\mathbf{r})$ (a.u.).

low density near the C1 atom. The distribution of the derivative potential does not coincide with the electron density distribution ρ_θ. This is the reason why the VCC of this mode is the smallest.

It is interesting to note that it is not necessary for the VCC of the mode which has large component on the carbons to be large.

VII. CONCLUSION

We present a new method of calculation of vibronic coupling constant, taking a JT molecule, cyclopentadienyl radical, as an example. It is confirmed that symmetry breaking at degenerate point and violation of Hellmann-Feynman theorem occur in the calculations based on a single Slater determinant. In order to overcome these difficulties, the electronic wave functions are calculated using generalized restricted Hartree-Fock (GRHF) and CASSCF methods, and the couplings are computed as matrix elements of the electronic operator of the vibronic coupling. Our result agrees well with the experimental and theoretical values by Applegate et al. A concept of vibronic coupling density is proposed in order to explain the order of magnitude of the coupling constant from view of the electronic and vibrational structures. It is found that the vibronic coupling of the JT-active mode is large when the frontier electron density ρ matches the one-electron electronic operator v_i. Furthermore it can illustrate the local properties of the coupling and enables us to control the interaction. This could open a way to the engineering of vibronic interactions. For instance, replacement by a heteroatom or introduction of a functional group for a molecule alters, the matching between the frontier electron density and the one-electron electronic operator.

[1] I. Bersuker, *The Jahn-Teller Effect and Vibronic Interactions in Modern Chemistry* (Plenum, New York, 1984).
[2] G. Fischer, *Vibronic Coupling: The Interaction Between the Electronic and Nuclear Motions* (Academic, London, 1984).
[3] I. Bersuker and V. Polinger, *Vibronic Interactions in Molecules and Crystals* (Springer-Verlag, Berlin, 1989).
[4] I. Bersuker, Chem. Rev. (Washington, D.C.) **101**, 1067 (2001).
[5] H. Jahn and E. Teller, Proc. R. Soc. London, Ser. A **161**, 220 (1937).
[6] L. Gribov and W. Orville-Thomas, *Theory and Methods of Calculation of Molecular Spectra* (Wiley, Chichester, 1988).
[7] T. Barckholtz and T. Miller, J. Phys. Chem. A **103**, 2321 (1999).
[8] B. Applegate, T. Miller, and T. Barckholtz, J. Chem. Phys. **114**, 4855 (2001).
[9] T. Kato and K. Hirao, Adv. Quantum Chem. **44**, 257 (2003).
[10] H. Hellmann, *Einführung in die Quantenchemie* (Franz Deuticke, Leipzig, 1937).
[11] R. Feynman, Phys. Rev. **56**, 340 (1939).
[12] R. Kuczkowski, J. Am. Chem. Soc. **87**, 5260 (1965).
[13] G. Liebling and H. McConnell, J. Chem. Phys. **42**, 3931 (1965).
[14] A. Carrington, H. Longuett-Higgins, R. Moss, and P. Todd, Mol. Phys. **9**, 187 (1965).
[15] M. Kira, M. Watanabe, and H. Sakurai, J. Am. Chem. Soc. **102**, 5202 (1980).
[16] P. Barker, A. Davies, and W. Tse, J. Chem. Soc., Perkin Trans. 2 **1980**, 941.
[17] G. Porter and B. Ward, Proc. R. Soc. London, Ser. A **303**, 139 (1968).
[18] R. Engleman and D. Ramsay, Can. J. Phys. **48**, 964 (1970).
[19] H. Nelson, L. Pasternack, and J. McDonals, Chem. Phys. **74**, 227 (1983).
[20] J. Yao, J. Fernandez, and E. Bernstein, J. Chem. Phys. **110**, 5174 (1999).
[21] J. Fernandez, J. Yao, and E. Bernstein, J. Chem. Phys. **110**, 5159 (1999).
[22] L. Yu, S. Foster, J. Williamson, M. Heaven, and T. Miller, J. Phys. Chem. **92**, 4263 (1988).
[23] L. Yu, J. Williamson, and T. Miller, Chem. Phys. Lett. **162**, 431 (1989).
[24] L. Yu, D. Cullin, J. Williamson, and T. Miller, J. Chem. Phys. **98**, 2682 (1993).
[25] P. Engelking and W. Lineberger, J. Chem. Phys. **67**, 1412 (1977).
[26] A. Liehr, Z. Phys. Chem., Neue Folge **9**, 338 (1956).
[27] L. Snyder, J. Chem. Phys. **33**, 619 (1960).
[28] W. Hobey and A. McLachlan, J. Chem. Phys. **33**, 1695 (1960).
[29] R. Meyer, F. Graf, T.-K. Ha, and H. Gunthard, Chem. Phys. Lett. **66**, 65 (1979).
[30] W. Borden and E. Davidson, J. Am. Chem. Soc. **101**, 3771 (1979).
[31] A. Szabo and N. Ostlund, *Modern Quantum Chemistry: Introduction to Advanced Electronic Structure Theory* (Macmillan, New York, 1982).
[32] M. Frisch, G. Trucks, H. Schlegel, G. Scuseria, M. Robb, J. Cheeseman, V. Zakrzewski, J. J. A. Montgomery, R. Stratmann, J. Burant et al., GAUSSIAN 98, Revision A.9, Pittsburgh PA, 1998.
[33] Cambridge Analytic Derivative Package (CADPAC), Issue 6.5, Cambridge, UK, 2001.
[34] W. Borden and E. Davidson, Acc. Chem. Res. **29**, 67 (1996).